Laser and Particle Beams (1995), *vol.* 13, *no.* 2, *pp.* 255–269
Printed in the United States of America

Application of Hartree–Fock theory of fluctuations to opacity calculation

By T. BLENSKI AND S. MOREL
IGA, Département de Physique, Ecole Polytechnique Fédérale de Lausanne, CH-1015 Lausanne, Switzerland

(Received 23 May 1994; revised 17 January 1995; accepted 19 January 1995)

The Hartree–Fock theory of fluctuations leading to simple formulae for configuration probabilities is used in a Detailed Configuration Accounting calculation of opacity in the case of an iron plasma. A direct Detailed Term Accounting method is also applied. The correlations of subshell occupation numbers, which are accounted for in the HF theory, show small effect on the theoretical spectrum corresponding to conditions of a recent measurement.

I. Introduction

In a previous paper (Blenski & Morel 1993), we described an approach to correlations of the subshell occupation numbers based on the Hartree–Fock (HF) theory of fluctuations. We present here the first results from our opacity program using this approach. Our work is in progress and our first calculations were intended to check the applicability of our method. Our opacity program is based on Detailed Configuration Accounting (DCA) which uses the HF correlation formula to calculate electron configuration probabilities. Our program also has a Detailed Term Accounting (DTA) option. This option is based on the direct simultaneous diagonalizations of the Hamiltonian and the angular momentum operators. We show as examples some results of our calculations in the case of an iron plasma at 20 eV temperature and at 0.01 density, which is not far from the conditions of a recent experiment (Da Silva *et al.* 1992). Our goal was to check whether our Detailed Configuration Accounting method works correctly. Taking into account the simplicity of the HF theory of fluctuations, this method seems to be a good tool in opacity calculation where a DCA approach is required.

Regarding DCA-DTA option, our objective is to verify whether our DCA method can be applied to opacity calculations when the term structure is taken into account. The DTA calculations reported in the literature (performed with the OPAL code, Iglesias *et al.* 1987), which demonstrated the importance of the term structure for some low temperature plasmas, are based on a statistical-mechanics method (activity expansion) which seems to be rather different compared to our approach. Let us stress again that our approach is consistent with the average atom approach to the plasma equilibrium and is probably one of the simplest methods which takes into account the detailed configurations. For this reason, we were interested in whether the results of our calculations show the redistribution of oscillator strengths predicted by Iglesias *et al.* (1987) and confirmed experimentally by Da Silva *et al.* (1992). Another approach using correlations to DCA calculations has also been proposed by Grimaldi and Grimaldi-Lecourt (1982) and Wilson (1993). A method similar to the present one but based on the density functional theory was introduced by Perrot (1988).

 0263-0346/95 $11.00 + .10

In our DTA option, we have used the direct diagonalization method, first proposed by Goldberg *et al.* (1986), since this method appeared to us to be the simplest one. Now, after the experience of our calculations, we think that this method cannot be directly applied to the full DTA calculations because of its matrix character and necessary restriction in the dimensions of the operator matrices. Perhaps it can still be a candidate for a DTA-UTA approach in which some transition arrays containing few lines are treated using Detailed Term Accounting, while others are accounted for by statistical methods (UTA-Unresolved Transition Array methods; Bauche *et al.* 1979, 1988).

The paper is organized as follows. We start with a derivation of the thermal average of the absorption cross section using the imaginary part of the dynamic electron polarizability (Section 2). Next we neglect the configuration interaction and introduce formally the configuration probability (Section 3). The formula used to calculate this probability is presented in the text, while all details of the HF theory at non-zero temperature and of the HF theory of fluctuations are described in Appendices A and B, respectively. The direct DTA diagonalization is briefly introduced in Section 4, while details of this method may be found in Appendix C. Finally, in Section 5, the numerical results are shown and discussed.

2. Thermal average of the absorption cross section

The thermal averaged atomic absorption cross section can be derived from the formula (Fetter & Walecka 1971; Grimaldi *et al.* 1985)

$$\sigma_a(\omega) = -\frac{4\pi\omega e^2}{3c}\, Im \int d\vec{r}\, d\vec{r}'\vec{r}\vec{r}'\chi^R(\vec{r},\vec{r}',\omega), \tag{1}$$

where $\chi^R(\vec{r},\vec{r}',\omega)$ is the Fourier transform of the retarded electron polarization (Fetter & Walecka 1971, §32)

$$\chi^R(\vec{r},\vec{r}',t-t') = -\frac{i}{\hbar}\, Tr\{\hat{P}[\hat{n}_H(\vec{r},t),\hat{n}_H(\vec{r}',t')]\}\theta(t-t'). \tag{2}$$

In equation (2), Tr denotes trace, $\hat{P}$ is the statistical operator, and $\hat{n}_H(\vec{r},t)$ is the electron density operator in the Heisenberg representation. $\theta(t-t')$ is the Heaviside function corresponding to the causality principle. The statistical operator has the form

$$\hat{P} = \frac{e^{-(\hat{H}-\mu\hat{N})/T}}{Tr\, e^{-(\hat{H}-\mu\hat{N})/T}}, \tag{3}$$

where $\hat{H}$ and $\hat{N}$ are the Hamiltonian and the electron number operator, respectively. Taking the Fourier transform of equation (2) and using the Lehmann representation (Fetter & Walecka 1971) leads to

$$Im\,\chi^R(\vec{r},\vec{r}',\omega) = -\pi(1-e^{-\hbar\omega/T})\sum_{n,m} P_n\langle n|\hat{n}(\vec{r})|m\rangle\langle m|\hat{n}(\vec{r}')|n\rangle\delta(\hbar\omega-(E_m-E_n)), \tag{4}$$

where $|n\rangle$ represent N-electron eigenstates of the Hamiltonian corresponding to the eigenvalues E_n. Eigenvalues of the statistical operator for these states are denoted P_n. The basis $|n\rangle$ is complete and contains free electron states.

Finally, we obtain for the absorption cross section

$$\sigma_a(\omega) = \frac{4\pi^2\omega e^2}{3c}(1-e^{-\hbar\omega/T})\sum_{n,m} P_n|D_{nm}|^2\delta(\hbar\omega-(E_m-E_n)), \tag{5}$$

with

$$D_{nm} = \int d\vec{r} \langle n | \hat{n}(\vec{r}) \cdot \vec{r} | m \rangle. \tag{6}$$

In the coordinate representation, $\hat{n}(\vec{r})$ has the form:

$$n(\vec{r}) = \sum_{k=1}^{N} \delta(\vec{r} - \vec{r}_k). \tag{7}$$

We see that our initial formula equation (1) already contains the correction for the stimulated emission.

The formula, equation (5), is exact. Now we make an approximation and neglect the configuration interactions. This allows to write for the bound-bound absorption cross section:

$$\sigma_a^{bb}(\omega) = \frac{4\pi^2 \omega e^2}{3c} (1 - e^{-\hbar\omega/T}) \sum_{n_c} P_{n_c} \sum_{i \in n_c} \frac{P_{n_c,i}}{P_{n_c}} \sum_{m_c} \sum_{j \in m_c} |D_{n_c m_c}|^2 \delta(\hbar\omega - (E_{m_c,j} - E_{n_c,i})). \tag{8}$$

In equation (8), n_c and m_c run over all initial and final bound electron configurations, respectively. i and j run over all N-electron eigenstates of the Hamiltonian in configurations n_c and m_c, respectively. The configuration is characterized by the subshells (in terms of the principal and the angular quantum numbers) occupation numbers. The configuration probability P_{n_c} is introduced formally in equation (8). At this moment, the only approximation we have done is to neglect the configuration interactions.

3. Detailed configuration accounting

We assume now that for each configuration, the relative probabilities for all initial eigenstates belonging to n_c are nearly equal; that is, we assume that in equation (8), $P_{n_c,i}/P_{n_c} = 1/N_S^{n_c}$ where $N_S^{n_c}$ is the number of these initial states, that is, the number of all its Slater determinants. We take into account, however, the exact positions of the lines (within the approximation neglecting the configuration interactions) and exact values of the oscillator strengths by diagonalization of the N-electron Hamiltonian for each initial and final configuration. We assume also that P_{n_c} can be calculated using the probability of the spherically symmetric fluctuations in the HF theory (Appendix B).

The configurations are introduced as follows. First, the fractional occupation numbers of the subshells in the self-consistent HFS atom will be cut to the nearest integers (Goldberg *et al.* 1986). We obtain in this way an electronic configuration which is called the most probable configuration. In the next step, we create different atomic configurations by moving electrons from one subshell to another (including ionization) and taking into account the Pauli principle. We create in this way all possible configurations of bound electrons, in ground and excited states. Each configuration n_0 is characterized by the set of (integer) deviations of the occupation numbers $\delta q_{n,l}^0$ with respect to the occupation numbers of the most probable configuration $\bar{q}_{n,l}$. We take as the probability of the n_0 configuration:

$$P_{n_0}[\delta q_{n_i,l_i}^0, i \in B] = \tilde{C}^{(B)} \exp\left[-\frac{1}{2} \sum_{j,k} \delta q_{n_j,l_j}^0 A_{n_j,l_j;n_k,l_k} \delta q_{n_k,l_k}^0 \right] \tag{9}$$

using the variances obtained in the HF theory of spherically symmetric fluctuations (Appendix B). $\tilde{C}^{(B)}$ is the normalization constant.

4. Detailed term accounting

In the diagonalization of the Hamiltonian and the angular momentum operators, two coupling schemes are applied: the intermediate and the LS (Russell-Saunders) couplings (Cowan 1981).

In the first case, we look for the common eigenstates $|n_c,i\rangle$ of the operators $\{\hat{J}^2,H\}$, where H is the Hamiltonian and $\hat{J}$ is the total angular momentum operator. As noted in Goldberg *et al.* (1986), the diagonalization may be performed in the subspace of eigenstates corresponding to the smallest non-negative value $M^{n_c}_{J,\min}$ of the operator J_z.

In the second case, we simultaneously diagonalize the operators $\{\hat{L}^2,\hat{S}^2,H\}$ with $\hat{L}$ and $\hat{S}$ being the orbital angular momentum and spin operators, respectively. Similarly, as in the case of the intermediate coupling, only the states corresponding to the subspace of the smallest non-negative eigenvalues $M^{n_c}_L = 0$ and $M^{n_c}_S = 0, \frac{1}{2}$ of the operators L_z and S_z, respectively, are to be considered. For details, see Appendix C.

5. Numerical results and conclusions

5.1. *Correlations of subshell occupation numbers*

The importance of interaction in the auto-correlations (i.e., in the diagonal terms, G^{-1}_{ii}; see equation (B14)) of subshell occupation numbers in the case of solid density iron has been presented in Blenski and Morel (1993). Let us recall that only in the case of the 3*d* subshell are the interactions with other subshells important, especially at low temperatures. The interactions of bound electrons with free electrons were less important than the interactions between bound electrons. We present numerical results which confirm this observation in figure 1. Let us remark here that it would be interesting to check the continuity

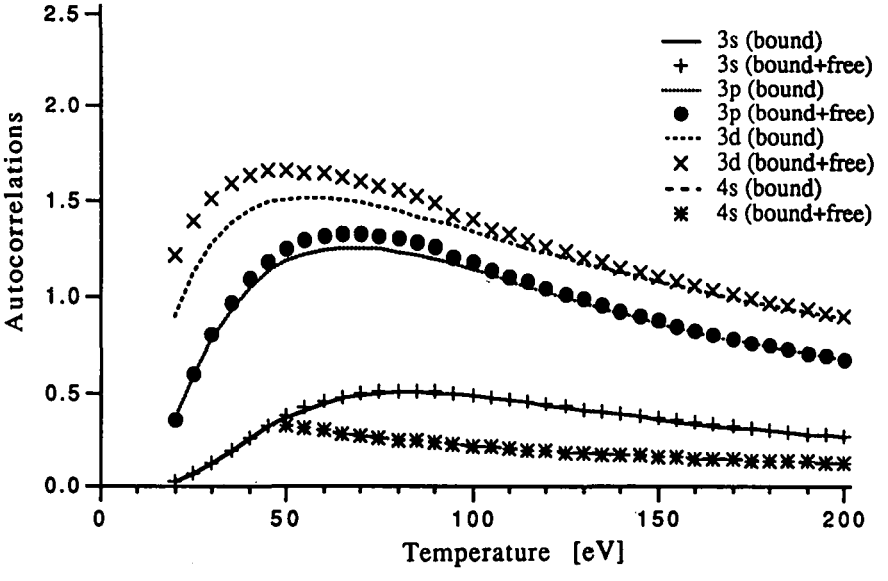

FIGURE 1. Autocorrelation versus temperature of the subshell occupation numbers for iron plasma of solid density. Effect of free electrons. The continuous lines correspond to the autocorrelations calculated with the interactions between bound electrons taken into account and with the neglected interactions between bound and free electrons. The points correspond to calculations with the inclusion of interactions between bound and free electrons.

of correlations in the case of pressure ionization (More 1985). Indeed, if the correlations between a bound level, which is close to be pressure-ionized, and the rest of the bound levels are important, then after the pressure ionization, when the mentioned level appears as a resonance in the free spectrum, we should find that the correlations between the free and bound spectrum are important. In the present calculations, however, the free levels were treated within the approximation such that only these parts of their wave functions, which are inside the Wigner-Seitz sphere, are taken into account. This problem needs a solution in the frame of a common formalism for bound and free electrons (Blenski & Cichocki 1992).

Figure 2 presents the ion charge distributions for solid density iron around the charge of the most probable atom for two temperature values, 50 and 100 eV. The distribution on the right corresponding to 50 eV shows a larger effect of the inclusion of interactions. At 50 eV, the $3d$ subshell occupation auto-correlation exhibits large dependence on interactions (Blenski & Morel 1993).

5.2. *Examples of DCA and DTA calculations in the case of iron plasma*

In the opacity program, we take into account only orbitals with a principal quantum number up to $n = 5$ and neglect states with higher n. We use average atom (AA) photoionization (bound-free) cross sections so the edge splitting is not included. AA inverse bremsstrahlung (free-free) cross sections are also taken. The line shapes are in the form of Voigt functions. The physical broadening mechanism includes electron impact, Stark and Doppler broadenings (Rozsnyai 1977). The results we present here are preliminary. We focus our attention on frequency-dependent spectra.

All calculations concern the case of iron at 20 eV temperature and at 0.01 g/cm^3 density. These parameters are not very far from the conditions of the Da Silva *et al.* (1992) experiment.

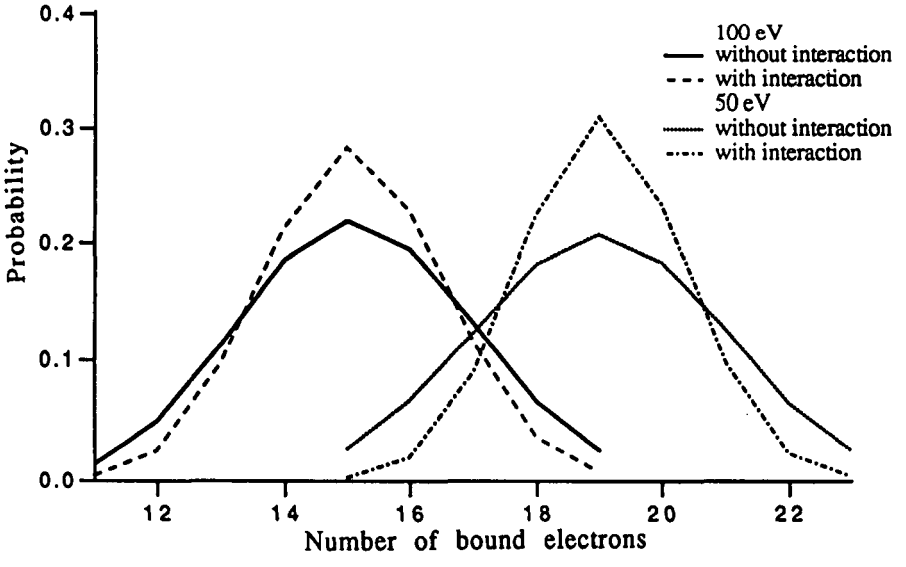

FIGURE 2. Distribution in the number of bound electrons with our probability model in the case of iron at solid density. The results for two temperature values are presented: 50 eV (right) and 100 eV (left). In both cases, the distributions obtained with and without interactions are presented.

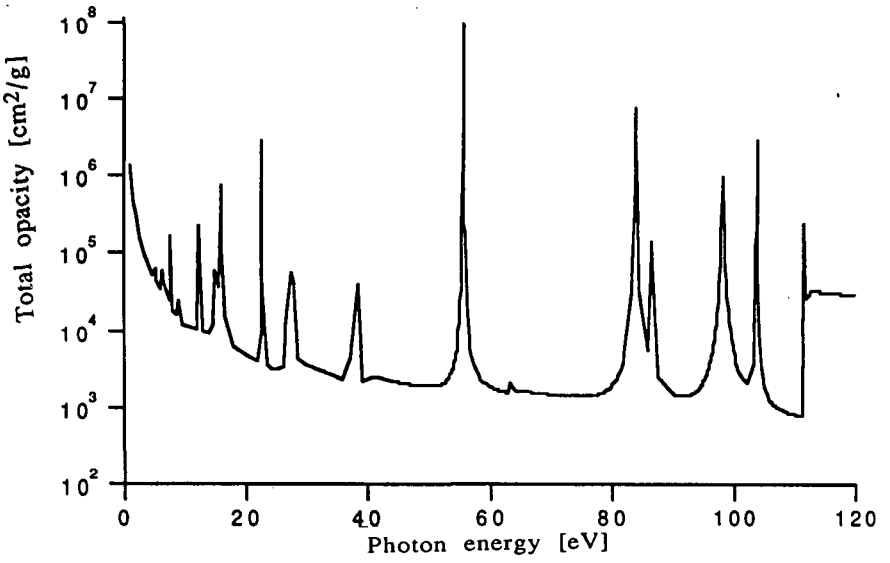

FIGURE 3. Total opacity for iron plasma at 20 eV temperature and at 0.01 g/cm^3 density. Independent electron model (average atom). Number of transitions bound-bound: 40.

Figure 3 displays photoabsorption versus photon energy obtained using the independent electron cross-section formula with the average atom wave functions and energies (i.e., only one average atom configuration with the fractional occupation numbers is used). There are 40 transitions and the strongest line comes from the nonhydrogenous $3p \rightarrow 3d$ transition. This line corresponds to 57 eV photon energy.

Figures 4 and 5 present results of the DCA calculations in which the term structure is neglected. The energy of each DCA line is taken as the difference between the total configuration average energies of the initial and final states. We notice that the DCA approximation redistributes the $3p \rightarrow 3d$ transitions symmetrically around the 60 eV photon energy. Both curves are similar, which means that the increase of the number of configurations has little impact on the final result.

Figures 6 and 7 present results of calculations in which some transition arrays (by transition array we mean all lines between two definite configurations) have been treated using the DTA approach. The criterion for the DTA treatment was that the dimensions of the diagonalized matrices be smaller than 200. We observed that both in the LS and in the intermediate coupling, only a part of the DCA lines was subject to the term splitting. This part was larger in the case of the LS splitting (about half of the DCA lines) since the criterion $M_L^{n_c} = 0$ and $M_S^{n_c} = 0, \frac{1}{2}$, in the LS case reduces more effectively the number of states than the criterion $M_{J,min}^{n_c} = 0, \frac{1}{2}$, in the intermediate case. Nevertheless, the number of lines even in the LS case was insufficient to fulfill the UTA structure present in figure 7 between 55 and 90 eV. The total Rosseland opacity increases from 4618 cm^2/g in the DCA calculation (figure 5) to the value 11302 cm^2/g in the case of the DTA-LS calculation (figure 7). We notice that the last value is smaller by at least a factor of 2 than the value obtained in DCA-UTA calculations (Blenski & Morel 1995). On the other hand, from the qualitative point of view, the spectra from both figures 6 and 7 confirm the observation made by Da Silva *et al.* (1992). We see the redistribution of the DCA lines situated around the 60 eV to the large UTA structure appearing in the DTA calculations between 55 and 90 eV.

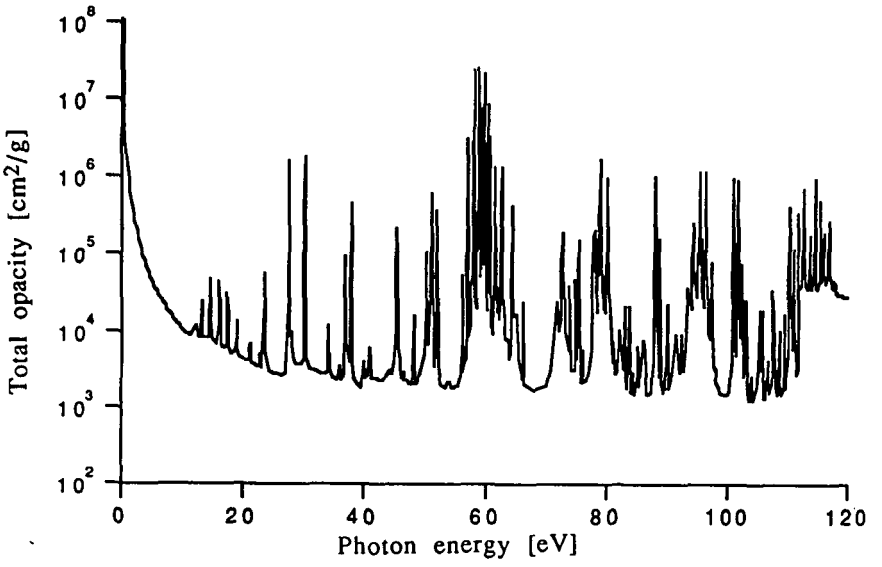

FIGURE 4. Total opacity for iron plasma at 20 eV temperature and at 0.01 g/cm^3 density. DCA model. Number of transitions bound-bound: 670. Number of initial configurations taken into account in the calculation: 29. Number of possible electron configurations: 37785.

Finally, an interesting question appears: What is the role of the interaction term in equation (B10) on the probability of configurations and on the calculated opacity spectrum? Figure 8 displays the result of the calculation in which the uncorrelated probabilities have been used (i.e., equation (B19)). Comparing figure 8 with figure 7, we see that in the ana-

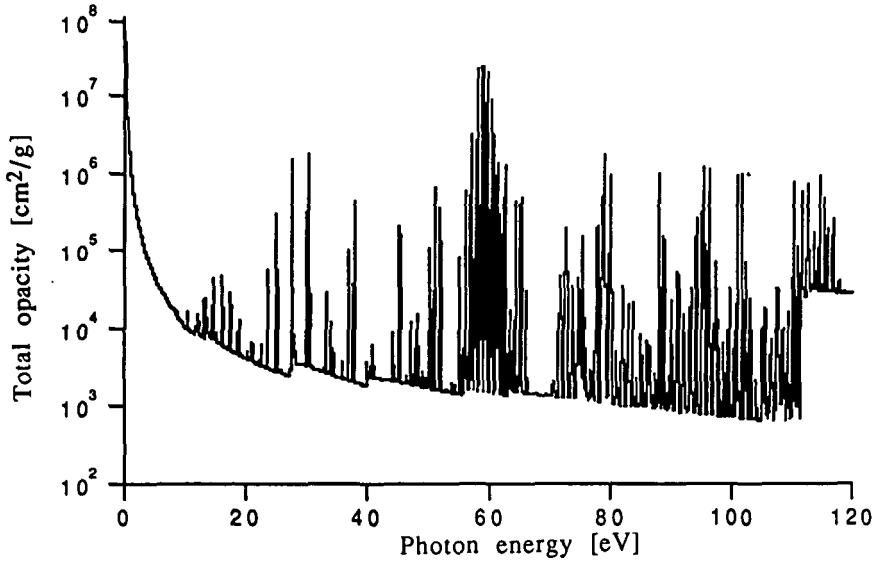

FIGURE 5. Total opacity for iron plasma at 20 eV temperature and at 0.01 g/cm^3 density. DCA model. Number of transitions bound-bound: 362517. Number of initial configurations taken into account in the calculation: 13079. Number of possible electron configurations: 37785.

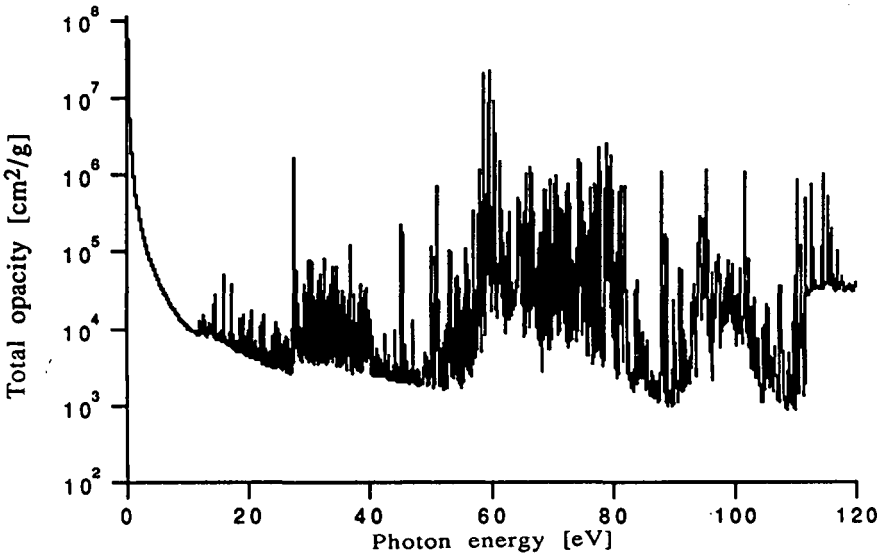

FIGURE 6. Total opacity for iron plasma at 20 eV temperature and at 0.01 g/cm^3 density. DTA model, intermediate coupling. Number of transitions bound-bound: 180310. Number of initial configurations taken into account in the calculation: 29. Number of possible electron configurations: 37785.

lyzed case, the role of interactions seems to be small since both spectra are very similar. The difference in the calculated Rosseland opacities in two cases was inferior to 6%. The reason for this behavior may be the fact that the subshell 3*d*, which is subject to large correlations with other subshells (Blenski & Morel 1993) at small temperatures, appears only as final state in important lines.

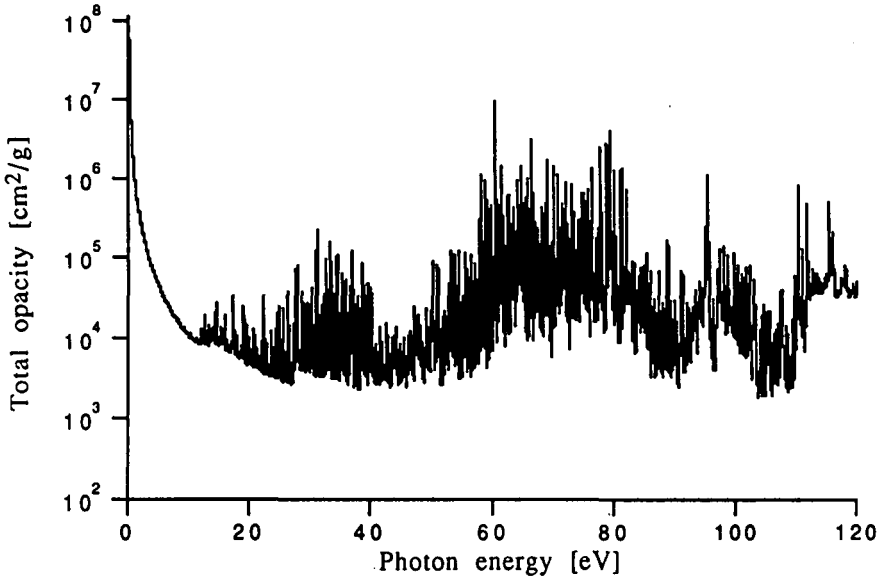

FIGURE 7. Total opacity for iron plasma at 20 eV temperature and at 0.01 g/cm^3 density. DTA model, LS coupling. Number of transitions bound-bound: 100741. Number of initial configurations taken into account in the calculation: 29. Number of possible electron configurations: 37785.

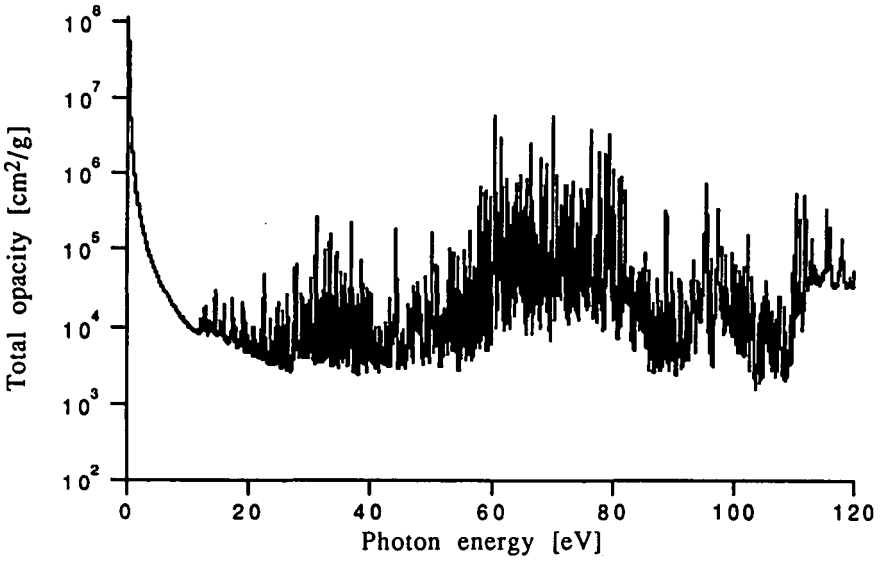

FIGURE 8. Total opacity for iron plasma at 20 eV temperature and at 0.01 g/cm^3 density. DTA model, intermediate coupling. The probabilities of configurations are calculated without interactions. Number of transitions bound-bound: 180310. Number of initial configurations taken into account in the calculation: 29. Number of possible electron configurations: 37785.

In conclusion, we state that the HF theory of fluctuation may be applied to DCA and DCA-DTA calculations of opacity spectra. We obtain qualitatively the main features observed in the experiment (Da Silva *et al.* 1992). The limitations of the DTA direct diagonalization method, which we have used, are responsible for too small number of lines in our calculations, which leads to the underestimation of the Rosseland mean opacity. The direct diagonalization method may be useful for small-Z atom calculation or as a supplement to a statistical UTA-type approach.

Acknowledgment

The authors would like to thank Drs. B. Cichocki and F. Grimaldi for discussions and critical comments. This research has been partially supported by the Swiss Federal Office for Science and Education (European Network "High Energy Density Matter"), "Union des Centrales Suisses d'Electricité" and Swiss National Science Fund.

REFERENCES

BAUCHE, J. *et al.* 1979 *Phys. Rev. A* **20**, 3183.

BAUCHE, J. *et al.* 1988 *Adv. Atom. Molec. Phys.* **23**, 131.

BLENSKI, T. & CICHOCKI, B. 1990 *Phys. Rev. A* **41**, 6973.

BLENSKI, T. & CICHOCKI, B. 1992 *Laser Part. Beams*, **10**, 303.

BLENSKI, T. & MOREL, S. 1993 *Nuovo Cimento A* **106**, 1781.

BLENSKI, T. & MOREL, S. 1995 in preparation.

COWAN, R.D. 1981 *The Theory of Atomic Structure and Spectra* (University of California Press, Berkeley).

CROWLEY, B.J.B. 1990 *Phys. Rev. A* **41**, 2179.

DA SILVA, L.B. *et al.* 1992 *Phys. Rev. Lett.* **69**, 438.

FELDERHOF, B.U. 1969 *J. Math. Phys.* **10**, 1021.

FETTER, A.L. & WALECKA, J.D. 1971 *Quantum Theory of Many-Particle Systems* (McGraw-Hill, New York).

GOLDBERG, A. *et al.* 1986 *Phys. Rev. A* **34**, 421.

GRIMALDI, F. & GRIMALDI-LECOURT, A. 1982 *J. Quant. Spectros. Radiat. Transfer* **27**, 373. (See also F. Grimaldi, In *Proceedings of Conferences on Radiative Properties of Hot Dense Matter*, Sarasota (1985, 1992).

GRIMALDI, F. *et al.* 1985 *Phys. Rev. A* **32**, 1063.

IGLESIAS, C.A. *et al.* 1987 *Ap. J.*, **322**, L45.

LANDAU, L. & LIFCHITZ, E. 1967 *Physique Statistique* (Editions Mir, Moscou).

MAHAN, G.D. & SUBBASWAMY, K.R. 1990 *Local Density Theory of Polarizability* (Plenum, New York).

MERMIN, N.D. 1963 *Ann Phys. (N.Y.)* **21**, 99.

MORE, R.M. 1985 *Adv. At. Mol. Phys.* **21**, 305.

ROZSNYAI, B.F. 1972 *Phys. Rev. A* **5**, 1137.

ROZSNYAI, B.F. 1977 *J. Quant. Spectros. Radiat. Transfer* **17**, 77.

PERROT, F. 1988 *Physica A* **150**, 357.

WILSON, B.G. 1993 *J. Quant. Spectrosc. Radiat. Transfer* **49**, 241.

APPENDIX A: Average atom

We start with an average atom (Rozsnyai 1972; Blenski & Cichocki 1990) submerged in a partially ionized plasma. The electron density of bound and free electrons is obtained via the Schrödinger states. The atomic potential is nonzero only inside the Wigner-Seitz sphere, which is neutral. The average atom results from thermal average over all electronic and ionic states of the plasma when overlapping of the ionic spheres is neglected (Crowley 1990). Another method leading to the average atom is the cluster expansion in the ionic configurations (Blenski & Cichocki 1992). The description of the thermal Hartree-Fock theory of electrons may be found in Mermin (1963), Felderhof (1969), and Thouless (1960, 1961). The Hartree-Fock equations, which result from minimization of the grand thermodynamic potential $\Omega(\rho)$ with respect to the electron density matrix ρ, are:

$$\tilde{\rho}_i \equiv \tilde{\rho}_{ii} = \frac{1}{e^{(\varepsilon_i-\mu)/T}+1}, \tag{A1}$$

$$\varepsilon_i \equiv \varepsilon_{ii} = t_{ii} + V_{ii} + \sum \langle in|v|in\rangle \tilde{\rho}_n, \tag{A2}$$

where ρ_i is the electron density matrix, t_{ii} is the kinetic energy, V_{ii} the potential energy:

$$V_{ii} = \left\langle i \left| \frac{-Ze^2}{|\vec{r}|} \right| i \right\rangle \tag{A3}$$

and the electron-electron interaction has the form:

$$\langle in|v|jm\rangle = \langle in|v_{ee}|jm\rangle - \langle in|v_{ee}|mj\rangle, \tag{A4}$$

where

$$v_{ee} = \frac{e^2}{|\vec{r}-\vec{r}'|}. \tag{A5}$$

In equations (A1–A2), the values of energy ε_i are measured with respect to the chemical potential. The wave-function basis used in the above formulas is that which diagonalizes the matrices ρ and γ (Mermin 1963). The one-electron states $|i\rangle$ describe here all solutions

to the Hartree-Fock self-consistent equations A1–A5. These states may be bound or free. In the fluctuation theory (Appendix B), the free electron wave function will be taken as different from the plane wave only inside the Wigner-Seitz sphere. The Hartree-Fock-Slater equations for the average atom are the same as equations (A1–A5), except that in equation (A4), the exchange term is replaced by an exchange-correlation potential. The model takes into account mean-field interactions of the bound and free electrons inside this sphere.

APPENDIX B: Fluctuations near the average atom equilibrium

The corrections to the density matrix, $\delta\tilde{\rho}_{ij}$, result in the following second order deviation of the grand thermodynamic potential, $\delta^2\Omega$, from its equilibrium value (Mermin 1963; Felderhof 1969):

$$\delta^2\Omega = \tfrac{1}{2}\sum \delta\tilde{\rho}^*_{ij}\langle ij|U|mn\rangle\delta\tilde{\rho}_{mn}, \tag{B1}$$

where

$$\langle ij|U|mn\rangle = \left(\frac{\varepsilon_i - \varepsilon_j}{\tilde{\rho}_i - \tilde{\rho}_j}\right)\delta_{im}\delta_{jn} + \langle in|v|jm\rangle, \tag{B2}$$

and where the summation runs over all electronic states, bound and free.

Equation (B1) shows that the fluctuations around the Hartree-Fock equilibrium are characterized by pairs of states rather than by occupations of levels. The matrix $\delta\rho$ is nondiagonal since $\delta\rho$ in general does not commute with the matrix ρ. We will, however, consider, in what follows, only $\delta\rho$ that are diagonal. They correspond to $\delta\rho$ which can be described in terms of fluctuations of the occupation numbers. One then has:

$$\langle ii|U|jj\rangle = \left(\frac{T}{\tilde{\rho}_i(1-\tilde{\rho}_i)}\right)\delta_{ij} + \langle ij|v|ij\rangle, \tag{B3}$$

and

$$\delta^2\Omega = \frac{1}{2}\sum_{i,j}\delta\tilde{\rho}_i\langle ii|U|jj\rangle\delta\tilde{\rho}_j, \tag{B4}$$

where

$$\delta\tilde{\rho}_i \equiv \delta\tilde{\rho}_{ii}. \tag{B5}$$

In the summation in equation (B3), the index belongs to bound (B) or free (F) spectrum. Further approximation is the assumed spherical symmetry of fluctuations. Using the spherical electronic waves functions leads to:

$$\delta\tilde{\rho}_i \equiv \delta\tilde{\rho}_{n_i,l_i,m_i,s_i}, \tag{B6}$$

and this approximation means that the corrections to the occupation numbers will depend only upon the principal n_i and angular l_i, quantum numbers:

$$\delta\tilde{\rho}_{n_i,l_i,m_i,s_i} = \delta\tilde{\rho}_{n_i,l_i}, \tag{B7}$$

that is, that the distribution among different magnetic and spin quantum numbers is uniform:

$$\sum_{i,j}\delta\tilde{\rho}_i\langle ij|v|ij\rangle\delta\tilde{\rho}_j = \sum_{\substack{n_i,l_i\\ n_j,l_j}}\delta\tilde{\rho}_{n_i,l_i}\delta\tilde{\rho}_{n_j,l_j}\sum_{\substack{m_i,s_i\\ m_j,s_j}}(\langle ij|v_{ee}|ij\rangle - \langle ij|v_{ee}|ji\rangle). \tag{B8}$$

These approximations lead to:

$$\frac{\delta^2\Omega}{T} = \frac{1}{T}\sum_{i,j}\delta\tilde{\rho}_i\langle ii|U|jj\rangle\delta\tilde{\rho}_j = \sum_{\substack{n_i,l_i\\n_j,l_j}}\delta\rho_{n_i,l_i}\delta\rho_{n_j,l_j}X_{ij}, \tag{B9}$$

with (Blenski & Morel 1993)

$$X_{ij} = \frac{1}{2(2l_i+1)}\left(\left(\frac{1}{\tilde{\rho}_{n_i,l_i}(1-\tilde{\rho}_{n_i,l_i})}\right)\delta_{n_i,n_j}\delta_{l_i,l_j} + \frac{e^2}{2T}\left[F^0(ij) - \frac{1}{2}\sum_{k=0}^{\infty}\left[\begin{pmatrix} l_i & k & l_j\\ 0 & 0 & 0\end{pmatrix}\right]^2 G^k(ij)\right]\right). \tag{B10}$$

We introduced the notation

$$\delta\rho_i = \delta\rho_{n_i,l_i} = 2(2l_i+1)\delta\tilde{\rho}_{n_i,l_i}. \tag{B11}$$

The Slater radial integrals and Wigner $3j$ coefficients are defined in the usual way (Cowan 1981):

Since we are interested in fluctuations of bound levels occupations, the above formula should be averaged over all possible fluctuations of free levels:

$$P[\delta\rho_i, i\in B] = \int_{-\infty}^{\infty}\cdots\int_{-\infty}^{\infty}\prod_{k\in F}d\delta\rho_k P[\delta\rho_i, i\in B,F]. \tag{B12}$$

Taking $[\delta\rho_i, i\in F]$ as varying from minus to plus infinity violates the Pauli exclusion principle. Let us note, however, that for higher values of $\delta\rho_i$, the probability will be very small and the changes introduced by this approximation may be negligible (Landau & Lifchitz 1967).

In practical calculations, the continuous free spectrum will be discretized. Let us introduce the following simplifying notation: The vector $\delta\rho_i\ i\in B,F$ will be denoted as $\delta\rho$. Its part corresponding to bound states, $\delta\rho_i$, $i\in B$, will have the index (1), $\delta\rho_{(1)}$, and its free part, $\delta\rho_i$; $i\in F$, the index (2), $\delta\rho_{(2)}$. This convention will also be applied to other vectors and to the matrix X and its inverse.

The integrations of equation (B12) can be performed analytically and we obtain:

$$P[\delta\rho_i, i\in B] = C^{(B)}e^{-G(\delta\rho_{(1)})/2}, \tag{B13}$$

$$G(\delta\rho_{(1)}) = \delta\rho_{(1)}X_{(1,1)}\delta\rho_{(1)} - \delta\rho_{(1)}X_{(1,2)}[X_{(2,2)}]^{-1}X_{(2,1)}\delta\rho_{(1)}. \tag{B14}$$

Equation (B14) gives the probability for a set of $\delta\rho_i$, $i\in B$, which represent corrections to average atom occupation numbers. Both excited states and states of different ion charge may be taken into account.

We may also consider fluctuations that preserve neutrality of the atom. Indeed, one may write:

$$P[\delta\rho_i, i\in B,F] = \tilde{C}^{(B,F)}\exp\left(-\frac{1}{T}\delta^2\Omega\right)\delta\left(\sum_{i\in B,F}\delta\rho_i\right), \tag{B15}$$

where δ denotes the Dirac delta.

The neutrality condition, standing in equation (B15), will be written using the vector D (defined as: $D_i = 1$, for $i\in B,F$), and again with our convention, $D_{(1)}$ and $D_{(2)}$. We then have:

$$\delta\rho D = \delta\rho_{(1)}D_{(1)} + \delta\rho_{(2)}D_{(2)} = 0. \tag{B16}$$

Performing the integration over free electron occupation numbers, we obtain:

$$P[\delta\rho_i, i \in B] = \tilde{C}^{(B)} \exp(-\tfrac{1}{2} G(\delta\rho_{(1)})), \tag{B17}$$

where G now has a third additional term:

$$G(\delta\rho_{(1)}) = \delta\rho_{(1)} X_{(1,1)} \delta\rho_{(1)} - \delta\rho_{(1)} X_{(1,2)} [X_{(1,2)}]^{-1} X_{(2,1)} \delta\rho_{(1)} + \frac{(D_{(1)} \delta\rho_{(1)} - D_{(2)} [X_{(2,2)}]^{-1} X_{(2,1)} \delta\rho_{(1)})^2}{D_{(2)} [X_{(2,2)}]^{-1} D_{(2)}}. \tag{B18}$$

Let us remark finally that if the interactions are totally neglected, we have the simple expression:

$$P[\rho_i, i \in B] = C'^{(B)} \prod_i e^{-[2(2l_i+1)(\rho_i - \rho_i^0)^2]/[2\rho_i(2(2l_i+1)-\rho_i)]}. \tag{B19}$$

APPENDIX C: Direct detailed term accounting

C1. Intermediate coupling

In this case, the N-electron states are completely determined by the quantum numbers $\{E_{n_c}, J_{n_c}, M_J^{n_c}\}$, where E_{n_c} denote eigenvalues of the operator H, J_{n_c} eigenvalues of the operator $\vec{J}^2$, and $M_J^{n_c}$ eigenvalues of the operator J_z of the states belonging to the configuration n_c. The summation over i and j in equation (8) is replaced by the summation over the quantum numbers $\{E_{n_c}, J_{n_c}, M_J^{n_c}\}$ and $\{E_{n_c}, J_{n_c}, M_J^{m_c}\}$. Only the diagonalization of the operators $\vec{J}^2$ and H in the subspace associated to the smallest value $M_{J,\min}^{n_c}$ should be considered. For that reason, only the matrix elements of the type $\langle E_{n_c}, J_{n_c}, M_{J,\min}^{n_c} | \sum \vec{r}_k | E_{m_c}, J_{m_c}, M_{J,\min}^{m_c} \rangle$ can be calculated. We shall express therefore the sum over $M_J^{n_c}$ and $M_J^{m_c}$ by these matrix elements.

The Wigner-Eckart theorem (Cowan 1981, p. 307) allows us to express the matrix elements of the dipole operator $\sum \vec{r}_k$ by the matrix elements of the reduced dipole tensor $\mathbf{P}^{(1)}$:

$$\left| \left\langle E_{n_c}, J_{n_c}, M_J^{n_c} \left| \sum_{k=1}^{N} \vec{r}_k \right| E_{m_c}, J_{m_c}, M_J^{m_c} \right\rangle \right|^2 = \sum_q \begin{pmatrix} J_{n_c} & 1 & J_{m_c} \\ -M_J^{n_c} & q & M_J^{m_c} \end{pmatrix}^2 |\langle E_{n_c}, J_{n_c} \| \mathbf{P}^{(1)} \| E_{m_c}, J_{m_c} \rangle|^2, \tag{C1}$$

where $\begin{pmatrix} J_{n_c} & 1 & J_{m_c} \\ -M_J^{n_c} & q & M_J^{m_c} \end{pmatrix}$ is the Wigner $3j$ coefficient (Cowan 1981, p. 142).

This Wigner $3j$ coefficient standing in equation (C1) is different from zero only if $-M_J^{n_c} + q + M_J^{m_c} = 0$. However, $M_{J,\min}^{n_c} = M_{J,\min}^{m_c}$, and the sum over q contains only $q = 0$ element. We therefore have

$$\left| \left\langle E_{n_c}, J_{n_c}, M_{J,\min}^{n_c} \left| \sum_{k=1}^{N} \vec{r}_k \right| E_{m_c}, J_{m_c}, M_{J,\min}^{m_c} \right\rangle \right|^2 = \begin{pmatrix} J_{n_c} & 1 & J_{m_c} \\ -M_{J,\min}^{n_c} & 0 & M_{J,\min}^{n_c} \end{pmatrix}^2 |\langle E_{n_c}, J_{n_c} \| \mathbf{P}^{(1)} \| E_{m_c}, J_{m_c} \rangle|^2. \tag{C2}$$

The sum over $M_J^{n_c}$ and $M_J^{m_c}$ in the matrix elements of the dipole operator becomes:

$$\sum_{M_J^{n_c}} \sum_{M_J^{m_c}} \left| \left\langle E_{n_c}, J_{n_c}, M_J^{n_c} \left| \sum_{k=1}^{N} \vec{r}_k \right| E_{m_c}, J_{m_c}, M_J^{m_c} \right\rangle \right|^2$$

$$= \sum_{M_J^{n_c}} \sum_{M_J^{m_c}} \sum_{q} \begin{pmatrix} J_{n_c} & 1 & J_{m_c} \\ -M_J^{n_c} & q & M_J^{m_c} \end{pmatrix}^2 \frac{\left| \left\langle E_{n_c}, J_{n_c}, M_{J,\min}^{n_c} \left| \sum_{k=1}^{N} \vec{r}_k \right| E_{m_c}, J_{m_c}, M_{J,\min}^{n_c} \right\rangle \right|^2}{\begin{pmatrix} J_{n_c} & 1 & J_{m_c} \\ -M_{J,\min}^{n_c} & 0 & M_{J,\min}^{n_c} \end{pmatrix}^2}. \quad \text{(C3)}$$

We now use the sum rule for the Wigner $3j$ coefficients (Cowan 1981, p. 145):

$$\sum_{m_1} \sum_{m_2} (2j_3 + 1) \begin{pmatrix} j_1 & j_2 & j_3 \\ m_1 & m_2 & m_3 \end{pmatrix} \begin{pmatrix} j_1 & j_2 & j_3' \\ m_1 & m_2 & m_3' \end{pmatrix} = \delta_{j_3, j_3'} \delta_{m_3, m_3'} \delta(j_1 j_2 j_3), \quad \text{(C4)}$$

where $\delta(j_1 j_2 j_3)$ equals 1 or 0 if j_1, j_2, and j_3 satisfy or do not satisfy the triangle inequalities, respectively. We finally obtain

$$\sum_{M_J^{n_c}} \sum_{M_J^{m_c}} \left| \left\langle E_{n_c}, J_{n_c}, M_J^{n_c} \left| \sum_{k=1}^{N} \vec{r}_k \right| E_{m_c}, J_{m_c}, M_J^{m_c} \right\rangle \right|^2$$

$$= \delta(J_{n_c} J_{m_c} 1) \cdot \frac{\left| \left\langle E_{n_c}, J_{n_c}, M_{J,\min}^{n_c} \left| \sum_{k=1}^{N} \vec{r}_k \right| E_{m_c}, J_{m_c}, M_{J,\min}^{n_c} \right\rangle \right|^2}{\begin{pmatrix} J_{n_c} & 1 & J_{m_c} \\ -M_{J,\min}^{n_c} & 0 & M_{J,\min}^{n_c} \end{pmatrix}^2}, \quad \text{(C6)}$$

and obtain for the bb absorption cross section the following results:

$$\sigma_a^{bb}(\omega) = \frac{4\pi^2 \omega e^2}{3c} (1 - e^{-\hbar\omega/T}) \sum_{n_c} \frac{P_{n_c}}{N_S^{n_c}} \sum_{m_c} \sum_{E_{n_c}, J_{n_c}} \sum_{E_{m_c}, J_{m_c}} \delta(J_{n_c} J_{m_c} 1)$$

$$\times \delta(\hbar\omega - (E_{m_c} - E_{n_c})) \frac{\left| \left\langle E_{n_c}, J_{n_c}, M_{J,\min}^{n_c} \left| \sum_{k=1}^{N} \vec{r}_k \right| E_{m_c}, J_{m_c}, M_{J,\min}^{n_c} \right\rangle \right|^2}{\begin{pmatrix} J_{n_c} & 1 & J_{m_c} \\ -M_{J,\min}^{n_c} & 0 & M_{J,\min}^{n_c} \end{pmatrix}^2}. \quad \text{(C7)}$$

Within the approximation that the configuration interactions are neglected, the N-electron states $|E_{n_c}, J_{n_c}, M_{J,\min}^{n_c}\rangle$ and $|E_{m_c}, J_{m_c}, M_{J,\min}^{m_c}\rangle$ can be expressed in the basis of Slater determinants belonging to the initial and final configuration, respectively:

$$|E_{n_c}, J_{n_c}, M_{J,\min}^{n_c}\rangle = \sum_{t=1}^{N_S^{n_c}} \langle \Phi_{n_c,t} | E_{n_c}, J_{n_c}, M_{J,\min}^{n_c} \rangle | \Phi_{n_c,t} \rangle = \sum_{t=1}^{N_S^{n_c}} \nu_t | \Phi_{n_c,t} \rangle,$$

$$|E_{m_c}, J_{m_c}, M_{J,\min}^{m_c}\rangle = \sum_{u=1}^{N_S^{m_c}} \langle \Psi_{n_c,u} | E_{m_c}, J_{m_c}, M_{J,\min}^{m_c} \rangle | \Psi_{m_c,u} \rangle = \sum_{u=1}^{N_S^{m_c}} \mu_u | \Psi_{m_c,u} \rangle. \quad \text{(C8)}$$

We recall that $N_S^{n_c}$ and $N_S^{m_c}$ denote the number of Slater determinants of the configurations n_c and m_c, respectively.

Substituting equation (C7) into equation (C6), we obtain

$$\sigma_a^{bb}(\omega) = \frac{4\pi^2\omega e^2}{3c}(1 - e^{-\hbar\omega/T}) \sum_{n_c} \frac{P_{n_c}}{N_S^{n_c}} \sum_{m_c} \sum_{E_{n_c},J_{n_c}} \sum_{E_{m_c},J_{m_c}} \delta(J_{n_c}J_{m_c}1)$$

$$\times \delta(\hbar\omega - (E_{m_c} - E_{n_c})) \frac{\left| \sum_{t=1}^{N_S^{n_c}} \sum_{u=1}^{N_S^{m_c}} \nu_t^* \mu_u \left\langle \Phi_{n_c,t} \left| \sum_{k=1}^{N} \vec{r}_k \right| \Psi_{m_c,u} \right\rangle \right|^2}{\begin{pmatrix} J_{n_c} & 1 & J_{m_c} \\ -M_{J,\min}^{n_c} & 0 & M_{J,\min}^{n_c} \end{pmatrix}^2}, \tag{C8}$$

where $\{\varphi_1^{n_c,t}, \ldots, \varphi_N^{n_c,t}\}$ and $\{\psi_1^{m_c,u}, \ldots, \Psi_N^{m_c,u}\}$ are the sets of one electronwave functions of the Slater determinants $\Phi_{n_c,t}$ and $\Psi_{m_c,u}$, respectively. Using the properties of the matrix elements involving the Slater determinants (Cowan 1981), we finally obtain:

$$\sigma_a^{bb}(\omega) = \frac{4\pi^2\omega e^2}{3c}(1 - e^{-\hbar\omega/T}) \sum_{n_c} \frac{P_{n_c}}{N_S^{n_c}} \sum_{m_c} \sum_{E_{n_c},J_{n_c}} \sum_{E_{m_c},J_{m_c}} \delta(J_{n_c}J_{m_c}1)$$

$$\times \delta(\hbar\omega - (E_{m_c} - E_{n_c})) \frac{\left| \sum_{t=1}^{N_S^{n_c}} \sum_{u=1}^{N_S^{m_c}} \nu_t^* \mu_u \langle \varphi_r^{n_c,t} | \vec{r} | \psi_r^{m_c,u} \rangle \right|^2}{\begin{pmatrix} J_{n_c} & 1 & J_{m_c} \\ -M_{J,\min}^{n_c} & 0 & M_{J,\min}^{n_c} \end{pmatrix}^2}. \tag{C9}$$

The matrix elements $\langle \varphi_r^{n_c,t} | \vec{r} | \psi_r^{m_c,u} \rangle$, containing one electron wave functions which are different in both configurations, are calculated using the formulae from Bethe and Salpeter (Cowan 1981, p. 253).

C2. LS coupling (Russell-Saunders)

In this case, the N-electron states are determined by the quantum numbers $\{E_{n_c}, L_{n_c}, S_{n_c}, M_L^{n_c}, M_S^{n_c}\}$ where E_{n_c} denote eigenvalues of the operator H, L_{n_c} eigenvalues of the operator L^2, S_{n_c} eigenvalues of the operator S^2, $M_L^{n_c}$ eigenvalues of the operator L_z, and $M_S^{n_c}$ eigenvalues of the operator S_z.

The summation over i and j in equation (8) is replaced by the sum over the quantum numbers E_{n_c}, L_{n_c}, S_{n_c}, $M_L^{n_c}$, $M_S^{n_c}$, E_{m_c}, L_{m_c}, S_{m_c}, $M_L^{m_c}$, and $M_S^{m_c}$. Only the diagonalization of the operators $\vec{L}^2$, $\vec{S}^2$, and H in the subspace corresponding to the smallest values of $M_L^{n_c} = 0$ and $M_S^{n_c} = 0, \frac{1}{2}$, is to be performed.

The sum over $M_L^{n_c}$ can be treated in the same manner as the sum over $M_J^{n_c}$ in Section C1. The sums over $M_S^{n_c}$ and over $M_S^{m_c}$ result in the factor $2S + 1$. Using the same notation as in the preceding section, we obtain for the absorption cross section in the LS coupling:

$$\sigma_a^{bb}(\omega) = \frac{4\pi^2\omega e^2}{3c}(1 - e^{-\hbar\omega/T}) \sum_{n_c} \frac{P_{n_c}}{N_S^{n_c}} \sum_{m_c} \sum_{E_{n_c},L_{n_c},S_{n_c}} \sum_{E_{m_c},L_{m_c},S_{m_c}} (2S_{n_c} + 1)$$

$$\times \frac{\delta(L_{n_c}L_{m_c}1)\delta(\hbar\omega - (E_{m_c} - E_{n_c}))}{\begin{pmatrix} L_{n_c} & 1 & L_{m_c} \\ -M_{L,\min}^{n_c} & 0 & M_{L,\min}^{n_c} \end{pmatrix}^2} \left| \sum_{t=1}^{N_S^{n_c}} \sum_{u=1}^{N_S^{m_c}} \nu_t^* \mu_u \langle \varphi_r^{n_c,t} | \vec{r} | \psi_r^{m_c,u} \rangle \right|^2. \tag{C10}$$

Since in this case we have only one possibility, $M_{L,\min}^{n_c} = 0$, we may directly use (Cowan 1981, p. 145)

$$\begin{pmatrix} L_{n_c} & 1 & L_{m_c} \\ 0 & 0 & 0 \end{pmatrix}^2 = \frac{max(L_{n_c}, L_{m_c})}{(2L_{n_c} + 1)(2L_{m_c} + 1)}. \tag{C11}$$